



Trajectory tracking control of quadcopter by designing Third order SMC Controller

Mebaye Belete Mamo^[1]

^[1]*AddisAbaba science and technology university, Ethiopia*
Mebaye.belete@aastu.edu.et

Abstract—This paper studies the modeling and control of quadcopter. It models the quadcopter nonlinear dynamics using Lagrange formalism and design controller for attitude (pitch & roll), heading & altitude tracking of the quadrotor. Mathematical modeling includes aerodynamic effects and gyroscopic moments. One Non-linear Control strategy, Third-Order Sliding Mode Control (TOSMC), based on a supertwisting algorithm has been proposed. The Controller has been implemented on the quadrotor physical model using Matlab/Simulink software. Finally, the performance of the proposed controller was demonstrated in the simulation study. The simulation results show excellent modeling and control performance.

Index Terms— TOSMC, Lagrange, Mathematical Modelling, Quadrotor, MATLAB/Simulink.

1. INTRODUCTION

Unmanned Aerial Vehicles (UAVs), especially multi-rotors, are becoming the mainstream in the civilian realm for performing a wide range of applications involving detection, recognition, and identification of different objects of interest. This is due to the advantages that this kind of aircraft presents in comparison to others like vertical takeoff and landing, hovering, the ability to follow a sharp trajectory, among others.

One of the most popular multirotors today is the quadrotor. This multirotor is highly nonlinear, under-actuated, and subject to disturbances and parameter uncertainties. Most of the research carried out on this platform has tackled the stabilization and trajectory tracking problems. There are several interesting robust flight controllers proposed for solving the stabilization problem, e.g. super twisting control algorithm [1], fuzzy control [2], a backstepping approach taking into account the actuator faults [3], among others.

Moreover, for the trajectory tracking problem, a feedback linearization controller with a high-order sliding mode observer [10], a backstepping control with a sliding mode observer [11], a combination of backstepping and sliding mode control [12], have been applied with satisfactory results.

Furthermore, linear adaptive methods such as model reference adaptive control have been suggested [13]. However, as for most linear methods, the achievable trajectory of the quadrotor is restricted due to the assumption of linearization. [14] proposed feedback controllers, which are based on a hierarchical control algorithm. The attitude is governed by employing a hybrid controller to overcome the well-known topological constraint, employed as a virtual input to stabilize the aircraft position, but still, there is a tracking problem.

The work in [15], designed a backstepping controller with integral action and suggested a single tool to design attitude, altitude, and position control. The modeling considered the rotor dynamics approximated to first-order transfer function but did not consider the aerodynamics disturbances.

Considering fault-tolerant control (FTC), various nonlinear algorithms including backstepping, sliding mode, and adaptive FTC approaches for quadrotor attitude and altitude tracking can be found in [16], [17], and the references therein. However, in many existing works in the literature, backstepping controllers have only been developed for the position (i.e., outer-loop) control of quadrotors [18].

In summary, the literature on quadrotor control ignores the aerodynamic effect, air disturbance, and gyroscopic moment in the dynamic modeling of the quadrotor. Besides, in the case of sliding mode controller implementation, it does not reduce both the control effort and chattering effect.

This paper uses a novel approach to address the above problems. It also designed a novel third-order SMC controller with minimum tracking error.

The paper is organized into five sections. In section 1, it introduces the quadrotor UAV. In Section 2, it models the physical system by considering the aerodynamic and gyroscopic effects. In Section 3, it designs second-order SMC based on the supertwisting algorithm. In Section 4, it presents the simulation results obtained from the control implementation of the physical system in the Simulink environment. Finally, in Section 5, it shows the control inputs and then concludes the work.

2. MATHEMATICAL MODELLING

In this section, a complete dynamical model of Quadrotor UAV is established using the Lagrange formalism.

2.1 Rotational Matrix

The orientation of the quadrotor is represented by Euler angles (pitch, roll, and yaw). To transform the body-fixed frame into the inertial frame; the z-y-x rotational matrix is considered [4].

To avoid the system singularities, it is important to assume the angle bound

$$-\frac{\pi}{2} < \varphi < \frac{\pi}{2}; -\frac{\pi}{2} < \theta < \frac{\pi}{2}; -\pi < \psi < \pi \quad (2.1)$$

$$R_{(x,\varphi)} = \begin{pmatrix} 1 & 0 & 0 \\ 0 & c\varphi & -s\varphi \\ 0 & s\varphi & c\varphi \end{pmatrix} \quad R_{(y,\theta)} = \begin{pmatrix} c\theta & 0 & s\theta \\ 0 & 1 & 0 \\ -s\theta & 0 & c\theta \end{pmatrix} \quad (2.2)$$

$$R_{(z,\psi)} = \begin{pmatrix} c\psi & -s\psi & 0 \\ s\psi & c\psi & 0 \\ 0 & 0 & 1 \end{pmatrix}$$

The Euler rotation about z-y-x or R_{xyz} is given by

$$R_{xyz} = R_{(z,\psi)} R_{(y,\theta)} R_{(x,\varphi)}$$

$$= \begin{pmatrix} c\psi c\theta & s\psi c\theta & c\psi s\theta & -s\psi s\theta & c\psi s\theta c\varphi + s\psi s\theta s\varphi \\ s\psi c\theta & c\psi c\theta & s\psi s\theta & -c\psi s\theta & s\psi s\theta c\varphi + c\psi s\theta s\varphi \\ -s\theta & s\theta & c\theta & 0 & c\theta c\varphi \end{pmatrix} \quad (2.3)$$

The studied quadrotor rotorcraft is detailed with their body- and inertial frames $F_b=(b,x^b,y^b,z^b)$ and $F_i=(G,x^G,y^G,z^G)$ respectively.

The model partitions naturally into translational and rotational coordinates [6]

$$\xi=(x,y,z) \in \mathbb{R}^3 \quad \eta=(\varphi,\theta,\psi) \in \mathbb{R}^3 \quad (2.4)$$

$\xi=(x,y,z)$ denotes the position vector of the center of mass of the quadrotor relative to the fixed inertial frame and $\eta=(\varphi,\theta,\psi)$ denotes the orientation of the quadrotor to the inertial frame. This is shown in Fig. 1 below

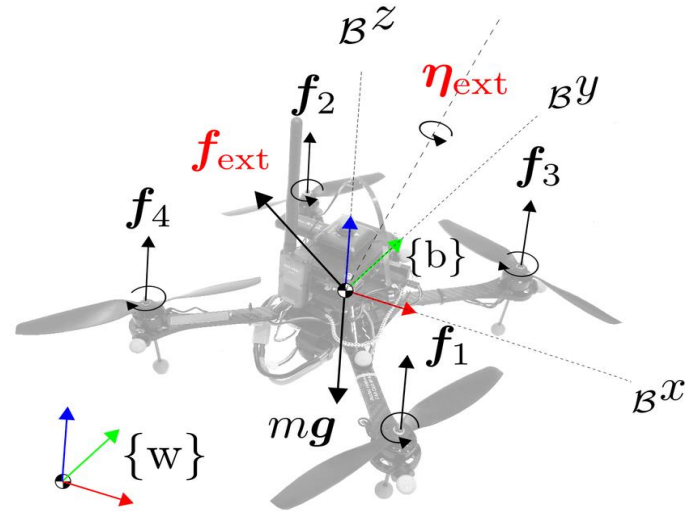


Figure 1 Typical quadrotor schematic diagram with the body and inertial frames [5]

2.2 Forces, Moments and Torques on Quadrotor

2.2.1 Thrust forces

Quadrotor has four propellers so that it produces four thrust forces.

$$F = \sum_{i=1}^4 F_i \quad (2.5)$$

$$F = F_1 + F_2 + F_3 + F_4 \quad (2.6)$$

2.2.2 Moments

Gyroscopic Moment: There are two gyroscopic torques, this is due to the motion of the propeller (M_{gp}) and the quadrotor body (M_{gb}) [11] given by:

$$M_{gp} = \sum_{i=1}^4 \Omega \wedge [0, 0, J_r (-1)^{i+1} w_i]^T \quad (2.7)$$

$$M_{gb} = \Omega \wedge J \Omega \quad (2.8)$$

$$J = \begin{pmatrix} I_{xx} & 0 & 0 \\ 0 & I_{yy} & 0 \\ 0 & 0 & I_{zz} \end{pmatrix} \quad (2.9)$$

Since the quadrotor geometry is symmetric, $I_{xy} = I_{xz} = I_{yx} = I_{yz} = I_{zx} = I_{zy} = 0$. Where Ω is the vector of angular velocity in a fixed earth frame.

$$\Omega = \begin{pmatrix} \dot{\phi} \\ \dot{\theta} \\ \dot{\psi} \end{pmatrix}$$

Aerodynamic friction moment: the quadrotor moves in the air, due to this it is subjected to aerodynamic friction. The torque caused by this the aerodynamic friction is called aerodynamic friction moment. It is given by:

$$M_a = \text{diag}(k_4, k_5, k_6) \begin{pmatrix} \dot{\phi}^2 & \dot{\theta}^2 & \dot{\psi}^2 \end{pmatrix}^T \quad (2.10)$$

$\text{diag}(k_4, k_5, k_6)$ are the aerodynamic friction coefficient and $\dot{\eta}^2$ are the angular velocity square vector for rotational dynamics.

2.2.3 Torques

Pitch torque

It is directly proportional to the difference of the thrust force generated by the second and fourth propellers ($F_4 - F_2$) [7-9].

$$\tau_\phi = l(F_4 - F_2) \quad (2.11)$$

Roll torque

It is directly proportional to the difference of the thrust force generated by the first and third propellers ($F_3 - F_1$) [7-9].

$$\tau_\theta = l(F_3 - F_1) \quad (2.12)$$

Yaw torque

which is directly proportional to the difference of thrust force generated by all propellers [7-9].

$$\tau_\psi = c(F_1 - F_2 + F_3 - F_4) \quad (2.13)$$

2.3 Modeling with Lagrange formalism

To obtain the quadrotor dynamics in terms of Lagrange, we use the Lagrange partial differential equation.

$$\frac{d}{dt} \frac{\partial L}{\partial \dot{q}} - \frac{\partial L}{\partial q} = F \quad (2.14)$$

Where $F = (F_\xi, \tau)$. We can calculate the translational and rotational components as follows

$$R_{xyz} \begin{pmatrix} 0 \\ 0 \\ \sum_{i=1}^4 F_i \end{pmatrix} - \begin{pmatrix} k_1 \dot{x} \\ k_2 \dot{y} \\ k_3 \dot{z} \end{pmatrix} = F_\xi = \begin{pmatrix} (c\phi s\theta c\psi + s\psi s\phi)u_1 - k_1 \dot{x} \\ (c\phi s\theta s\psi - s\theta c\psi)u_1 - k_2 \dot{y} \\ (c\phi c\theta)u_1 - k_3 \dot{z} \end{pmatrix} \quad (2.15)$$

$$\begin{pmatrix} \tau_\phi \\ \tau_\theta \\ \tau_\psi \end{pmatrix} - M_a - M_{gp} - M_{gb} = \tau = \begin{pmatrix} \tau_\phi - J_r \dot{\Omega}_r \dot{\theta} - (I_{zz} - I_{yy}) \dot{\theta} \dot{\psi} - k_4 \dot{\phi}^2 \\ \tau_\theta + J_r \dot{\Omega}_r \dot{\phi} - (I_{xx} - I_{zz}) \dot{\phi} \dot{\psi} - k_5 \dot{\theta}^2 \\ \tau_\psi - (I_{yy} - I_{xx}) \dot{\theta} \dot{\phi} - k_6 \dot{\psi}^2 \end{pmatrix} \quad (2.16)$$

Computing the Lagrange partial differential equation for all six generalized coordinates, get the following differential equations

$$\ddot{x} = (c\phi s\theta c\psi + s\psi s\phi) \frac{u_1}{m} - \frac{k_1}{m} \dot{x} \quad (2.17)$$

$$\ddot{y} = (c\phi s\theta s\psi - s\theta c\psi) \frac{u_1}{m} - \frac{k_2}{m} \dot{y} \quad (2.18)$$

$$\ddot{z} = (c\phi c\theta) \frac{u_1}{m} - \frac{k_3}{m} \dot{z} - g \quad (2.19)$$

$$\ddot{\phi} = \frac{\tau_\phi}{I_{xx}} - \frac{J_r \dot{\Omega}_r}{I_{xx}} \dot{\theta} - \frac{(I_{zz} - I_{yy})}{I_{xx}} \dot{\theta} \dot{\psi} - \frac{k_4}{I_{xx}} \dot{\phi}^2 \quad (2.20)$$

$$\ddot{\theta} = \frac{\tau_\theta}{I_{yy}} + \frac{J_r \dot{\Omega}_r}{I_{yy}} \dot{\phi} - \frac{(I_{xx} - I_{zz})}{I_{yy}} \dot{\phi} \dot{\psi} - \frac{k_5}{I_{yy}} \dot{\theta}^2 \quad (2.21)$$

$$\ddot{\psi} = \frac{\tau_\psi}{I_{zz}} - \frac{(I_{yy} - I_{xx})}{I_{zz}} \dot{\theta} \dot{\phi} - \frac{k_6}{I_{zz}} \dot{\psi}^2 \quad (2.22)$$

3. CONTROL SYSTEM DESIGN

3.1 THIRD ORDER SLIDING MODE

CONTROLLER

3.1.1 Super-twisting algorithm

Consider once more the dynamical system of relative degree 1 and suppose that

$$\dot{\sigma} = h(t, x) + g(t, x)u \quad (3.1)$$

$$\phi = \int U dt + k |\sigma|^{2/3} \text{sign}(\sigma) \quad (3.2)$$

Where k a is a positive constant

Furthermore, assume that for some positive constants C,

$$K_M, K_m, U_M, q$$

$$\left| \dot{h} + U_M \dot{g} \right| \leq C, \theta \leq K_m \leq g(t, x) \leq K_M, \left| \frac{h}{g} \right| < q U_M, 0 < q < 1 \quad (3.3)$$

Then the control signal becomes

$$U = -\lambda |\phi|^{\frac{1}{2}} \text{sign}(\phi) + u \quad \dot{u} = \begin{cases} -u, & \text{for } |u| > U_M \\ -\text{asign}(\phi), & \text{for } |u| < U_M \end{cases} \quad (3.4)$$

Theorem: with $K_m \alpha > C$ and λ sufficiently large, the controller (3.3) guarantees the appearance of a 2-sliding mode $\sigma = \dot{\sigma} = 0$ in the system, which attracts the trajectories in finite time. The control u enters in a finite time segment $[-U_M, U_M]$ and stays there. It never leaves the segment, if the initial value is inside at the beginning. A sufficient (very crude!) condition for the validity of the theorem is

$$\lambda > \frac{\sqrt{\frac{2}{(K_m \alpha - C)(K_m \alpha + C)K_M(1+q)}}}{K_m^2(1-q)} \quad (3.5)$$

Proof

3.1.1.1 Design of Sliding mode control for altitude (z)

The state-space equation for altitude is as follows

$$\begin{aligned} \dot{x}_5 &= x_6 \\ \dot{x}_6 &= (c\varphi c\theta) \frac{u_1}{m} - \frac{k_3}{m} x_6 - g \end{aligned} \quad (3.6)$$

Then the linear sliding surface form as $\sigma = ce + \dot{e}$ $c > 0$, if c is larger then the sliding dynamics decays rate is larger.

Where $e = x_5^d - x_5$ and $\dot{e} = \dot{x}_5^d - \dot{x}_5$. By select c be 3, then the sliding surface become

$$\sigma = 3e + \dot{e} \quad (3.7)$$

Then computing $\dot{\sigma}$ get

$$\dot{\sigma} = 3\dot{x}_5^d - \dot{x}_6 + \ddot{x}_5^d - (c\varphi c\theta) \frac{u_1}{m} + \frac{k_3}{m} x_6 + g \quad (3.8)$$

$$\phi = \int U dt + k |\sigma|^{\frac{2}{3}} \text{sign}(\sigma) \quad (3.8)$$

From the above 3.7, we assign

$$h(t, x) = 3x_5^d - x_6 + \ddot{x}_5^d + \frac{k_3}{m} x_6 + g \text{ and}$$

$$g(t, x) = -\frac{(c\varphi c\theta)}{m}$$

3.1.1.2 Design of Sliding mode control for attitude (φ, θ)

For φ

The state-space equation for pitch is as follows

$$\begin{aligned} \dot{x}_7 &= x_8 \\ \dot{x}_8 &= a_1 u_2 + a_2 \bar{\Omega}_r x_{10} + a_3 x_{10} x_{12} - k_4 a_1 x_8^2 \end{aligned} \quad (3.9)$$

Then the linear sliding surface form as $\sigma = ce + \dot{e}$ $c > 0$, if c is larger then the sliding dynamics decays rate is larger.

Where $e = x_7^d - x_7$ and $\dot{e} = \dot{x}_7^d - \dot{x}_7$. By select c be 3, then the sliding surface become

$$\sigma = 3e + \dot{e} \quad (3.10)$$

Then computing $\dot{\sigma}$ gets

$$\dot{\sigma} = 3\dot{x}_7^d - 3x_8 + \ddot{x}_7^d - a_2 \bar{\Omega}_r x_{10} - a_3 x_{10} x_{12} + k_4 a_1 x_8^2 - a_1 u_2 \quad (3.11)$$

$$\phi = \int U dt + k |\sigma|^{\frac{2}{3}} \text{sign}(\sigma) \quad (3.12)$$

From the above equation, we assign

$$h(t, x) = 3x_7^d - 3x_8 + \ddot{x}_7^d - a_2 \bar{\Omega}_r x_{10} - a_3 x_{10} x_{12} + k_4 a_1 x_8^2$$

$$\text{and } g(t, x) = -a_1$$

For θ

The state-space equation for the roll is as follows

$$\begin{aligned} \dot{x}_9 &= x_{10} \\ \dot{x}_{10} &= a_4 u_3 + a_5 \bar{\Omega}_r x_8 + a_6 x_8 x_{12} - k_5 a_4 x_{10}^2 \end{aligned} \quad (3.13)$$

Then the linear sliding surface form as $\sigma = ce + \dot{e}$ $c > 0$, if c is larger, then the sliding dynamics decays rate is

larger. Where $e = x_9^d - x_9$ and $\dot{e} = \dot{x}_9^d - \dot{x}_9$. By select c be 3, then the sliding surface become

$$\sigma = 3e + \dot{e} \quad (3.14)$$

Then computing $\dot{\sigma}$ get

$$\dot{\sigma} = 3\dot{x}_9^d - 3\dot{x}_{10} + \ddot{x}_9^d - a_5 \bar{\Omega}_r x_8 - a_6 x_8 x_{12} + k_5 a_4 x_{10}^2 - a_4 u_3 \quad (3.15)$$

$$\phi = \int U dt + k |\sigma|^{2/3} \text{sign}(\sigma) \quad (3.16)$$

From the above equation, we assign

$$h(t, x) = 3x_9^d - 3x_{10} + \ddot{x}_9^d - a_5 \bar{\Omega}_r x_8 - a_6 x_8 x_{12} + k_5 a_4 x_{10}^2$$

and $g(t, x) = -a_4$

3.1.1.3 Design of Sliding mode control for heading (ψ)

The state-space equation for yaw is as follows

$$\begin{aligned} \dot{x}_{11} &= x_{12} \\ \dot{x}_{12} &= a_8 x_{10} x_8 - k_6 a_7 x_{12}^2 + a_7 u_4 \end{aligned} \quad (3.17)$$

Then the linear sliding surface form as $\sigma = ce + \dot{e}$ $c > 0$, if c is larger, then the sliding dynamics decay rate is larger.

Where $e = x_{11}^d - x_{11}$ and $\dot{e} = \dot{x}_{11}^d - \dot{x}_{11}$. By select c be 3, then the sliding surface becomes

$$\sigma = 3e + \dot{e} \quad (3.18)$$

Then computing $\dot{\sigma}$ we get

$$\dot{\sigma} = 3\dot{x}_{11}^d - 3\dot{x}_{12} + \ddot{x}_{11}^d - a_8 x_{10} x_8 + k_6 a_7 x_{12}^2 - a_7 u_4 \quad (3.19)$$

$$\phi = \int U dt + k |\sigma|^{2/3} \text{sign}(\sigma) \quad (3.20)$$

From the above equation, we assign

$$h(t, x) = 3x_{11}^d - 3x_{12} + \ddot{x}_{11}^d - a_8 x_{10} x_8 + k_6 a_7 x_{12}^2$$

and $g(t, x) = -a_7$

3.2 Designed control system scheme block diagram

A diagram of the proposed control approach can be seen in Fig.2. The diagram clearly illustrates the implementation of

the control system designed on the quadrotor physical system.

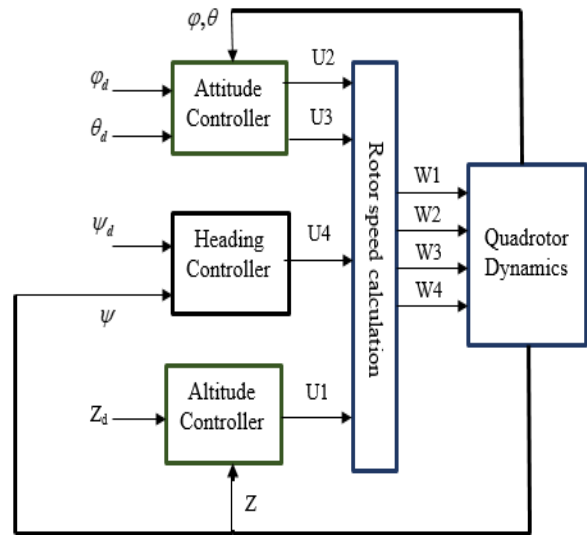


Figure 2 Control system scheme block diagram

3.3 Reference or desired values for tracking

$$\begin{cases} z_d = 0.5 + t \\ \phi_d = 0.174 \sin(t) \\ \theta_d = 0.174 \sin(t) \\ \psi_d = 0.174 \sin(t) \end{cases} \quad (3.21)$$

3.4 Calculated Controller parameters for tracking

The controller parameters listed below in Table 1 are calculated based on the above theorem.

TABLE I. Tracking problem controller parameters for sliding mode control

Variables/states	λ for Super-twisting SMC	α for Super-twisting SMC
Z(altitude)	100	15
Pitch(phi)	20	8
Roll (theta)	20	8
Yaw (psi)	20	8

4. Simulation results and Analysis

4.1 Parameters used for simulation

TABLE II Physical parameters for quadrotor [11]

Parameter	Value and unit
Arm Length(l)	0.5m
Total mass	0.5 kg
Quadrotor mass moment of inertia (I)	diag (0.005,0.005,0.01) kgm ²
Motor inertia (Jr)	2.8385*10 ⁻⁵ N.m/rad/s ²
Lift Coefficient (b)	2.984*10 ⁻⁵
Drag Coefficient(d)	3.3*10 ⁻⁷
Aerodynamic friction Coefficients (K _{1,2,3})	0.3729
Translational drag Coefficients (K _{4,5,6})	5.56*10 ⁻⁴
Gravitational acceleration(g)	9.81 m/s ²

4.2 Simulation graphs and Analysis

In this section, numerical simulations are carried out on the quadrotor system to validate the control performance of the proposed sliding mode control. For simulation purposes, the parameters listed in Table 2 are used.

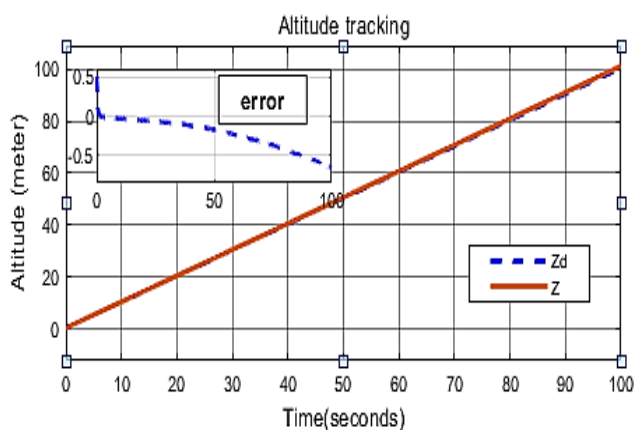


Figure 3 Altitude tracking controller performance using third-order SMC

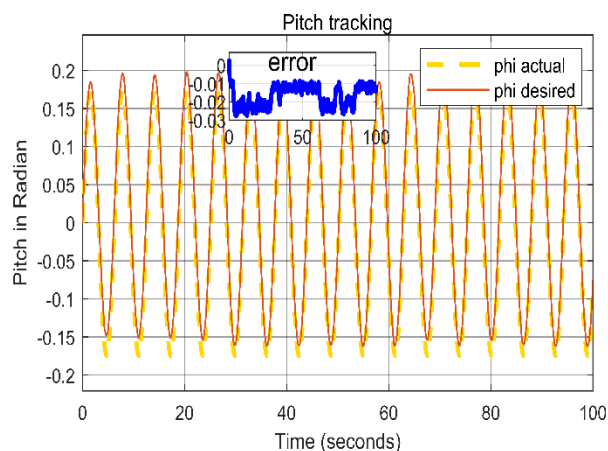


Figure 4 Pitch Tracking controller performance using third-order SMC

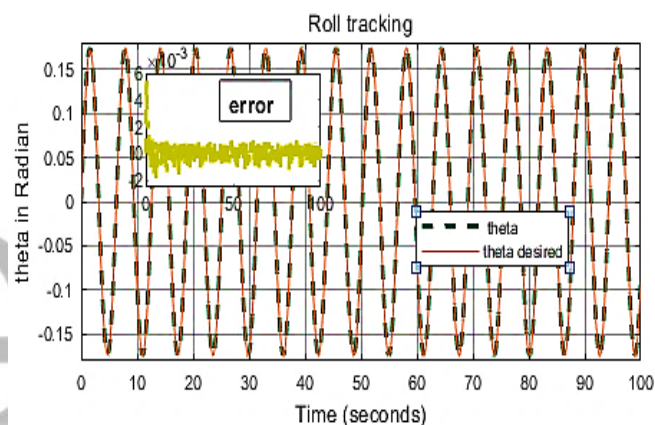


Figure 5 Roll tracking controller performance using third-order SMC

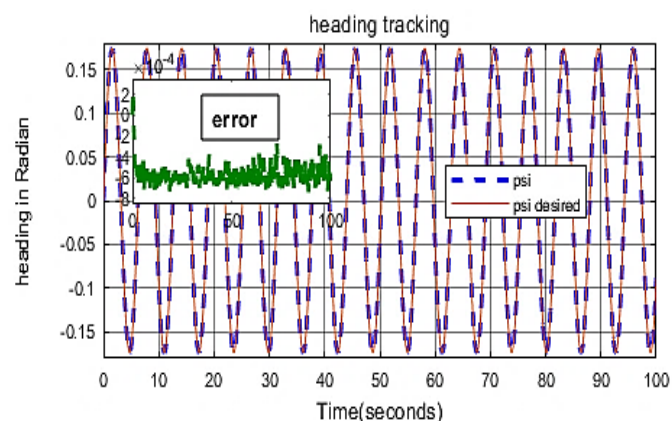


Figure 6 Yaw (heading) regulation controller performance using third-order SMC

The overall results are shown in Fig. 3, Fig. 4, Fig. 5, and Fig. 6, respectively. Fig.3 demonstrates the tracking performance of altitude, which is shown that the response of the quadrotor can follow the desired value as closely. Fig. 4,

Fig. 5, and Fig. 6 show the tracking performances of the three Euler angles, i.e., pitch, roll, and yaw, respectively. It shows that the quadrotor tracks the reference values for three Euler angles as closely as possible with minimum error.

It can be seen from the above simulation results that the proposed third-order sliding mode control is effective and accurate.

4.3 3D tracking using third-order super twisting SMC

1.Regular helix tracking

In this section, the helix tracking performance of the designed controller is demonstrated using three controlled variables. The variables are pitch, heading, and altitude. The variables selection among the four candidates is based on one from altitude, one from attitude, and one from heading. The desired trajectory is a regular helix generated from these parametric equations below. The base of the regular helix is an ellipse.

$$\begin{cases} xd = \varphi_d = 4 \sin(t) \\ yd = \psi_d = 5 \cos(t) \\ zd = z_d = 2 + t \end{cases} \quad (3.22)$$

x_d , y_d and z_d are the desired trajectories in the x-axis, y-axis, and z-axis respectively.

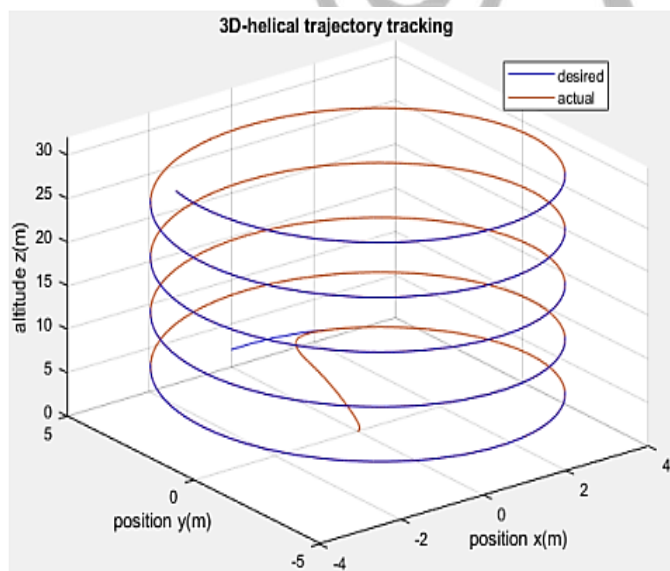


Figure 7 3D regular helical trajectory tracking using second-order SMC

In Fig.7, the result shows the tracking controller performance of the designed pitch, heading, and altitude controller on three-dimensional space. As seen from the three-dimensional

plot, the quadrotor has given the mission to track desired the three-dimensional trajectory indicated by the blue solid line described using the above parametric equations. As expected, the designed controllers for the three variables enable the quadrotor to track perfectly the desired three-dimensional trajectory.

2. Oblique helix tracking

In this section, the oblique helix tracking performance of the designed controller is demonstrated using the three controlled variables. The variables are roll, heading, and altitude. The variables selection among the four candidates is based on one from altitude, one from attitude, and one from heading. The desired trajectory is an oblique helix generated from the parametric equations below.

$$\begin{cases} xd = \theta_d = 5t \\ yd = \psi_d = 5 \cos(t) \\ zd = z_d = t \end{cases} \quad (3.23)$$

x_d , y_d and z_d are the desired trajectories in the x-axis, y-axis, and z-axis respectively.

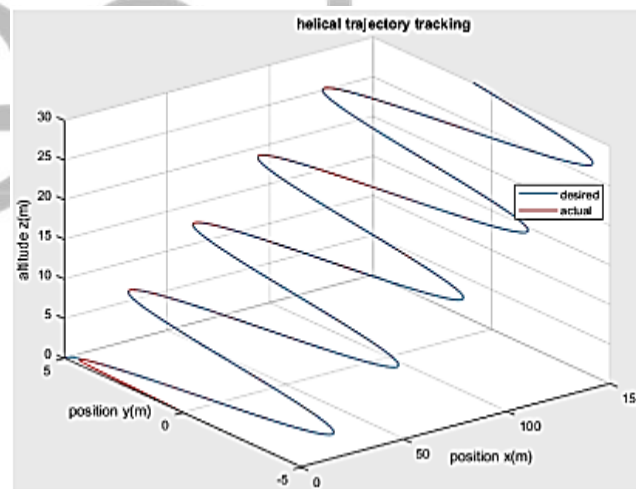


Figure 8 3D oblique helical trajectory tracking using second-order SMC

In Fig.8, the result shows the tracking controller performance of the designed roll, heading, and altitude controller on three-dimensional space. As seen from the three-dimensional plot, the quadrotor has given the mission to track the desired three-dimensional trajectory indicated by the blue solid line described by the above parametric equations. As expected, the designed controllers for the three variables enable the quadrotor to track perfectly the desired three-dimensional trajectory.

4.5 Third-order SMC controller performance measures

In this section, the designed third-order SMC controller performance for tracking is measured in terms of the performance index. Performance indexes are used to measure the controller's effectiveness and accuracy. In this case, the designed controller performance is measured in terms of integral square error (ISE), integral absolute error (IAE), integral time square error (ITSE), and mean square error (MSE) performance indexes.

These indexes' numerical values are tabulated in the table below.

TABLE III Higher-order SMC controller performance measures

Controlled variable	Performance measure indexes			
	ISE	IAE	ITSE	MSE
Altitude	0.04	0.15	0.00074	0.017
pitch	0.001	0.0034	0.0006	0.0003
Roll	0.002	0.0069	0.00001	0.0006
Yaw	0.002	0.0003	0.00005	0.0003

As we have seen from Table 3 that all performance measures numerical values are less than 0.05. This indicates the designed controller is highly effective and accurate in trajectory tracking.

Conclusion

In this paper, the nonlinear dynamic model of the quadrotor is derived using Lagrange formalism. The model contains two parts namely translational and rotational dynamics (Euler-angle dynamics). The nonlinear model includes the gyroscopic moments induced due to the rotational motion of the quadrotor body & propellers mounted on rotor. Besides, the aerodynamic friction moment & force are considered in the modeling. After the derivation of the dynamic model, a nonlinear control strategy (third-order SMC) based on a super-twisting algorithm is designed.

To verify the performance and efficiency of the controller, a simulation is done via Matlab/Simulink. Besides, four performance indexes are implemented to test the effectiveness and accuracy of the designed controller. Third order SMC is designed for four output-controlled variables separately. The controlled variables are altitude, pitch, roll, and yaw. The third-order SMC is implemented on the physical system for tracking problems. The controller is very effective; it can track the desired trajectory with fast & smooth response and good stability as shown from both simulation and performance index measures. Overall, the third-order SMC controller designed for the quadrotor for tracking is effective and has excellent performance.

References

- [1] L. Derafa, L. Fridman, A. Benallegue, and A. Ouldali, "Super twisting control algorithm for the four rotors helicopter attitude tracking problem," in Variable Structure Systems (VSS), 2010 11th International Workshop on, 2010, pp.62–67. [Online]. Available :<http://ieeexplore.ieee.org/stamp/stamp.jsp?arnumber=5544726>
- [2] A. Rabhi, M. Chadli, and C. Pegard, "Robust fuzzy control for stabilization of a quadrotor" in Advanced Robotics (ICAR), 2011 15th International Conference on, 2011, pp. 471–475. [Online]. Available: <http://ieeexplore.ieee.org/stamp/stamp.jsp?arnumber=6088629>
- [3] H. Khebbache, B. Sait, F. Yacef, and Y. Soukkou, "Robust stabilization of a quadrotor aerial vehicle in presence of actuator faults," International Journal of Information Technology, Control and Automation, vol. 2, no. 2, 2012, pp. 1–13.
- [4] P. Johan From, J. Tommy Gravdahl, K. Ytterstad Pettersen, Vehicle Manipulator System, Verlag, London: Springer, 2014.
- [5] Atheer L. Salih, M. Moghavvemi, Haider A. F. Mohamed, Khalaf Sallom Gaeid Modelling and PID Controller Design for a Quadrotor Unmanned Air Vehicle, IEEE, 2010.
- [6] D. Lee, H. Jin Kim, and S. Sastry, "Feedback linearization vs. adaptive sliding mode control for a quadrotor helicopter," International Journal of Control Automation and Systems, vol. 3, no. 7, pp. pp. 419-428, 2009.
- [7] O. Gherouat, D. Matouk, A. Hassam, and F. Abdessemed, "Modeling and Sliding Mode Control of a Quadrotor Unmanned Aerial Vehicle," J. Automation and Systems Engineering, vol. 10, no. 3, pp. 150-157, 2016.
- [8] Abraham Villanueva, B. Castillo-Toledo, and Eduardo Bayro-Corrochano, "Multi-mode Flight Sliding Mode Control System for a Quadrotor," in 2015 International Conference on Unmanned Aircraft Systems (ICUAS), Denver, Colorado, USA, June 2015.
- [9] Yi Kui, Gu Feng, Yang Liying, He Yuqing, Han Jianda, "Sliding Mode Control for a Quadrotor Slung Load System," in Proceedings of the 36th Chinese Control Conference, Dalian, China, July 26-28, 2017.
- [10] A. Benallegue, A. Mokhtari, and L. Fridman, "Feedback linearization and high order sliding mode observer for a quadrotor UAV" in Variable Structure Systems, 2006. VSS'06. International Workshop on, 2006, pp. 365–372. [Online]. Available:<http://ieeexplore.ieee.org/stamp/stamp.jsp?arnumber=1644545>
- [11] T. Madani and A. Benallegue, "Sliding mode observer and backstepping control for a quadrotor unmanned aerial vehicles," in American Control Conference, 2007. ACC '07, 2007, pp. 5887–

5892. [Online]. Available: [http://ieeexplore .ieee.org/ stamp /stamp.jsp?arnumber=4282548](http://ieeexplore.ieee.org/stamp/stamp.jsp?arnumber=4282548)

[12] S. Stevanovic, J. Kasac, and J. Stepanic, "Robust tracking control of a quadrotor helicopter without velocity measurement," in 23rd International DAAAM Symposium, Vienna, Austria, vol. 23, 2012, pp. 595–600.

[13] B. Whitehead and S. Bieniawski. Model Reference Adaptive Control of a Quadrotor UAV. In Guidance Navigation and Control Conference 2010, Toronto, Ontario, Canada, 2010. AIAA.

[14] Samir Bouabdallah, "Design and Control of Quadrotors with Application to Autonomous Flying", MSc thesis Zurich January 2007, DOI: 10.5075/epfl-thesis-3727 · Source: OAI article available at [http://www .Research.gate.net/publication/37439805](http://www.Research.gate.net/publication/37439805)

[15] S. Bouabdallah, "Design and Control of Quadrotors with Application to Autonomous Flying," MSc thesis, Dept. Autonomous system Eng., Aboubekr Belkaid Univ. Tlemcen, Algérie, 2007.

[16] R. C. Avram, X. Zhang, and J. Muse, "Nonlinear adaptive fault-tolerant quadrotor altitude and attitude tracking with multiple actuator faults," IEEE Transactions on control systems technology, vol. 26, pp. 701–707, March 2018

[17] S. Mallavalli and A. Fekih, "A fault-tolerant control design for actuator fault mitigation in quadrotor UAVs," in 2019 American Control Conference (ACC), pp. 5111–5116, July 2019

[18] M. E. Antonio-Toledo, E. N. Sanchez, A. Y. Alanis, J. Florez, and M. A. Perez-Cisneros, "Real-time integral backstepping with sliding mode control for a quadrotor UAV," IFAC-Papers Online, vol. 51, no. 13, pp. 549 –554, 2018. 2nd IFAC Conference on Modelling, Identification, and Control of Nonlinear Systems MICNON 2018.

APPENDICES

Mathematical calculation of control performance index

$$ISE = \int e^2(t)dt$$

$$IAE = \int |e(t)|dt$$

$$ITSE = \int te^2(t)dt$$

$$MSE = \frac{\int e(t)}{t}$$